Ain Shams University

Ain Shams Engineering Journal

www.elsevier.com/locate/asej
www.sciencedirect.com

ENGINEERING PHYSICS AND MATHEMATICS

# A hybrid Fuzzy C-Means and Neutrosophic for jaw lesions segmentation

**Mutasem K. Alsmadi**

*Department of MIS, College of Applied Studies and Community Service, University of Dammam, Saudi Arabia*

Received 13 November 2015; revised 23 February 2016; accepted 16 March 2016

**KEYWORDS**

Automatic segmentation;
Jaw panoramic X-ray image;
Neutrosophy;
Fuzzy C-Means clustering algorithm

**Abstract** It is really important to diagnose jaw tumor in its early stages to improve its prognosis. A differential diagnosis could be performed using X-ray images; therefore, accurate and fully automatic jaw lesions image segmentation is a challenging and essential task. The aim of this work was to develop a novel, fully automatic and effective method for jaw lesions in panoramic X-ray image segmentation. The hybrid Fuzzy C-Means and Neutrosophic approach is used for segmenting jaw image and detecting the jaw lesion region in panoramic X-ray images which may help in diagnosing jaw lesions. Area error metrics are used to assess the performance and efficiency of the proposed approach from different aspects. Both efficiency and accuracy are analyzed. Specificity, sensitivity and similarity analyses are conducted to assess the robustness of the proposed approach. Comparing the proposed approach with the Hybrid Firefly Algorithm with the Fuzzy C-Means, and the Artificial Bee Colony with the Fuzzy C-Means algorithm, the proposed approach produces the most identical lesion region to the manual delineation by the Oral Pathologist and shows better performance (FP rate is 6.1%, TP rate is 90%, specificity rate is 0.9412, sensitivity rate is 0.9592 and similarity rate is 0.9471).



## 1. Introduction

The mandible and maxilla (jaw) like other bones suffer from hundreds of generalized and localized lesions and neoplasms. Some of these lesions or tumors arise from the dental formative tissues, and therefore, it is called odontogenic which can be divided according to its development stage or tissues from which the tumor arose. Lesions or neoplasms arising from non-dental formative tissues are called non-odontogenic.

Inflammatory cysts are considered as one of the most common odontogenic and non-odontogenic jaw lesions followed by dentigerous cyst. In a total of 7412 oral lesions, Khosravi et al. found that radicular inflammatory cysts are the most common jaw lesions accounting for 35.12% of the total odontogenic cysts reported in his study [1].

Although osteosarcoma is a rare neoplasm, its early detection is very important to improve the prognosis as the survival of patients with osteosarcoma is usually less than 5 years [2,3]. Therefore, diagnosing jaw lesions and its early detection is one of the important challenges in oral health care [4,5].

E-mail addresses: mksalsmadi@gmail.com, mkalsmadi@uod.edu.sa

Peer review under responsibility of Ain Shams University.

ELSEVIER Production and hosting by Elsevier

http://dx.doi.org/10.1016/j.asej.2016.03.016



Please cite this article in press as: Alsmadi MK, A hybrid Fuzzy C-Means and Neutrosophic for jaw lesions segmentation, Ain Shams Eng J (2016), http://dx.doi.org/10.1016/j.asej.2016.03.016

Radiography is one of the most helpful and common diagnostic tools available to dental practitioners. X-rays usage as a standard diagnostic procedure is well established in the profession. It is important to get as much as possible diagnostic information from X-ray images. A differential diagnosis could be performed using X-ray images. Conventional films are used commonly in radiologic examination to evaluate jaw cysts and odontogenic tumors [6].

X-ray imaging is easy, convenient to use and reproducible method. The equipment is relatively cheap compared with other advanced imaging modalities. The images are easy to read once the observer is trained. They are also simple to store and retrieve. Diagnosis could be performed as soon as the image is taken [7].

White has introduced the Oral Radiographic Deferential Diagnosis (ORAD) program that is based on a questionnaire that was designed to evaluate the clinical and radiographic features of patients with intra-bony lesions using Bayes' theorem [8]. The aim of ORAD program was to assist in lesions identification. Ninety-eight jaw lesions were described by many features such as their prevalence and distribution by race, sex, age, and the presence of pain, size, number, and location of lesions, association with teeth, locularity, expansion, contents, borders and impact on adjacent teeth. There is a menu of 16 questions to characterize a specific lesion [8]. Other authors stated that practitioners may need training on feature recognition to be able to use diagnostic aids or "expert systems" such as ORAD [9].

A list of the lesions is introduced as output in order of their estimated probability. In addition, an estimate of the match extent between the lesion and the appearance of each lesion in the knowledge base is calculated. Preliminary tests indicate that ORAD is useful in assisting clinicians in formulating a differential diagnosis [10].

Radiologists usually analyze X-ray images by extracting features from the border of the lesion, internal structures, locularity, disiographic placement and resorption of the teeth [11].

Many steps are required to evaluate radiopaque jaw lesion. The first and most important step is to categorize the lesion by its attenuation, and its location with respect to the tooth. These observations are essential for the evaluation of any type of jaw lesion. Then it will be easy to create a proper differential diagnosis. Perilesional halo, growth pattern, bone expansion, and margin as well as the type of lesion – whether it is sclerotic, has ground-glass attenuation, or is mixed lytic and sclerotic are all important features that narrow the differential diagnosis. To explore the "terra incognita" of radiopaque jaw lesions it is important to be aware of the associated clinical features and their demographic distribution, as well as the radiologic approach [12].

The radiologists will be frequently consulted to evaluate a variety of jaw lesions or may incidentally encounter these lesions on routine patient's checkup. It is important to have a diagnostic approach pattern when faced with an unknown jaw lesion. Specific cardinal and additional radiographic criteria on plain film studies are important for differential diagnosis. The location with regard to the adjacent tooth structures within the jaw Cardinal and the density of the lesion are basic radiographic criteria. Other criteria in the jaw lesions evaluation are morphological characteristics, demarcation, periosteal, cortical involvement and soft tissue changes [13].

Lesions could be categorized into two types, namely well-defined and poorly-defined. A well-defined lesion is a tumor representing a distinct radiolucency with a corticated margin. In a poorly defined lesion, the border is readily identified but is not corticated. A diffuse border is characterized by a margin that could not be distinguished and the transitional zone between the lesion and unaffected bone is wide and indistinct. The internal structures indicate the type of trabeculations [14].

Some jaw lesions have characteristic radiographic appearance such as ameloblastoma which usually appear as a multilocular cyst like lesion of the jaw (honeycomb), while osteosarcoma appears usually as sunray radiopacity [2]. On the other hand, myxoma is described as delicate filamentous structures that tend to be angular and form square, rectangular or triangular compartments. Some studies called this feature "tennis racquet" appearance. The internal structures are evaluated with reference to these trabeculations [15].

It is important to provide dentists with the tools that help them to assess their own accuracy at least for common diagnostic problems. A major step in improving dentist's diagnostic accuracy is to identify features on X-ray images correctly and accurately [16,17].

Normally, one of the main participants in the image diagnostic process is the human observer. Diagnostic accuracy varies among dentists themselves when viewing X-ray images. A decision support system that helps in the diagnosing process is needed to improve their image diagnostic accuracy.

One of the effective clustering methods is the Fuzzy C-Mean (FCM). The method was developed in 1973 by Dunn [18] and enhanced by Bezdek in 1981 [19]. FCM is used widely as a clustering method in the pattern recognition field. It is also used in image analysis in the stage of image segmentation.

Shen et al. proposed an extension to the traditional FCM clustering algorithm. This extension depends on using the neighborhood attraction (NA). NA is dependent on the relative location and features of neighboring pixels. This would help to improve the segmentation performance. A Neural Network model is used to optimize the degree of attraction [20].

Some problems that cannot be solved by fuzzy logic approach can be solved using Neutrosophic logic. This approach can be beneficial to many fields, such as cancer diagnosis, weather forecasting, political elections and sporting events. Fuzzy logic cannot handle indeterminate conditions very well. Neutrosophy, on the other hand, introduces an indeterminacy set to deal with such conditions [20].

Anuradha and Sankaranarayanan [17] proposed a technique for mouth cancers detection utilizing a morphological mathematical watershed algorithm, this approach preserves the edge details, the marker controlled watershed is used for tumor segmentation purpose, and then the marker controlled watershed segmentation algorithm was compared with the watershed segmentation, and the marker controlled watershed has better results with 92.55% speed and 90.25% accuracy than the watershed segmentation with 91% speed and 85.20% accuracy.

Anuradha and Sankaranarayanan [21] presented a system for the segmentation and classification of abnormal and normal oral cancer images. This approach was carried out in three steps. Images are digitized and used as input image. Then, image processing is carried out for noise removal, after that image is segmented and features are extracted for tumor

Please cite this article in press as: Alsmadi MK, A hybrid Fuzzy C-Means and Neutrosophic for jaw lesions segmentation, Ain Shams Eng J (2016), http://dx.doi.org/10.1016/j.asej.2016.03.016

identification. The sensitivity and specificity were calculated using the Confusion Matrix, sensitivity equals 92.85% and Specificity equals 92.30% were obtained.

Anuradha and Sankaranarayanan [22] proposed an oral cancer detection system; it works by preprocessing images using Linear Contrast Stretching for noise removal, and then Watershed Segmentation is utilized. Because of Watershed segmentation problems, Marker Controlled Watershed segmentation is utilized, and Marker Controlled watershed segmentation decreases the over segmentation problem. The Improved Marker Controlled Watershed Segmentation algorithm obtains better segmentation result (higher speed) with or without linear contrast stretching of the image. The Processing Speed is calculated before stretching and after stretching. The speed of Watershed Segmentation is 87% (without stretching) and 91% (after Stretching); the speed of Marker Controlled Watershed was 90% (without stretching), and was 92.55% (after Stretching). The Improved Marker Controlled Watershed Segmentation achieved 90.5% speed (without stretching) and 92.6% (after Stretching).

Maghsoudi et al. [23] proposed an intelligent system based on artificial neural networks. This proposed system used 120 patient images, 120 for training process and 30 for testing and validation, and four features were extracted and used for diagnosis of mouth legions. This work indicated that artificial neural network when employed in the diagnostic systems provided a powerful approach for prediction and diagnosis of dental and oral diseases.

Nurtanio et al. [24] presented a segmentation system for cyst or tumor cases from dental panoramic images. They utilized the active contour models for the segmentation process by converting the colored images into gray images, and the active contour models (snake) provides a solution for number of visual problems, which includes detection of lines, edges and subjective contours. The segmentation with this model can be utilized for tumor lesion and cyst on oral panoramic images with high accuracy rate (99.67%).

Neutrosophy is a branch of approach that studies the origin, nature, and scope of neutralities, as well as their interactions with different ideational spectra [26,27]. Neutrosophic logic is a branch that generalizes fuzzy logic, and deals with paradoxes, contradictions, antitheses, antinomies [28]. It is based on the proposition that $t$ true, $i$ indeterminate, and $f$ false. $t$, $i$, $f$ are real values from the ranges $T$, $I$, $F$, with no restrictions on them. Examples on the indeterminate conditions are presidential election, sport games, weather forecast, etc [25].

Fuzzy C-Mean algorithm is very popular and robust clustering algorithm, and it obtains the data membership degrees by minimizing the cost function iteratively, while keeping the sum of the cluster membership degrees over each data equals 1. The FCM algorithm is the generalized form of the classical K-means algorithm, and is used in pattern classification, data mining, machine learning, etc. The proposed NFCM is the generalized form of the FCM method, and this approach may be applicable in many related areas [25].

The rest of this paper is organized as follows: Section 2 explains materials and methods used. Section 3 evaluates and discusses the obtained Results using proposed approach and other segmentations methods. Section 4 concludes the paper.

## 2. Materials and methods

The proposed Panoramic jaw's X-ray image segmentation approach consists of four phases that were carried out automatically, namely; Speckle reduction, image enhancement, a novel clustering approach (NFCM) is proposed here. Fig. 1 below shows the four phases of the proposed approach.

### 2.1. Speckle reduction

Determining the region of interest is not applicable to the jaw's images, due to the small lesion area compared to the constructions present in the panoramic jaw's X-ray image (fat, connective tissue, teeth and muscles). This work was applied on the whole jaw's X-ray image instead of the region of interest, and median filter of size $m = 3 * 3$ was applied to remove and reduce the speckle noise [29]. Median filters are most popular among the other filters because they provide excellent speckle reduction abilities for certain types of speckle noise compared with other filters such as linear smoothing filters of similar size [30].

### 2.2. NFCM for lesion detection

This work utilizes a new clustering approach (NFCM) that groups and clusters jaw's X-ray image pixels into background region and lesion region.

#### 2.2.1. Fuzzy C-Means clustering algorithm

Fuzzy C-Means (FCM) is a strong clustering method which permits one data piece to belong to two or more clusters [25,27,31,32]. The method relies on minimizing the objective function as follows:

$$J_m = \sum_{i=1}^{n}\sum_{j=1}^{c} u_{ij}^{m}\|x_i - c_j\|^2, 1 \leqslant m < \infty \quad (1)$$

where $m$ is any real number greater than 1 which represents the fuzziness exponent, $u_{ij}$ denote the membership of $x_i$ in cluster $J$, $x_i$ and $c_j$ denote the $i$th data point and cluster center of $J$, $\|\cdot\|$ is a norm representing the match between the data point and the cluster center [25]. Iterative optimization was the method used to achieve fuzzy partitioning using the objective function

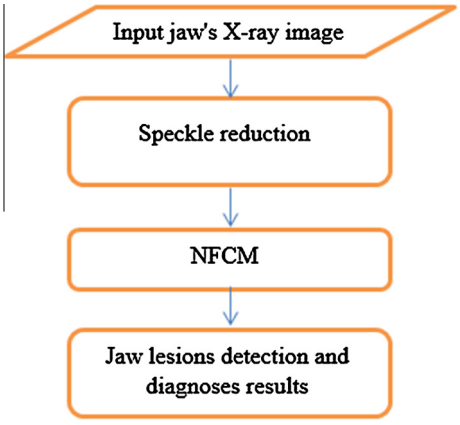


**Figure 1** The four phases of the proposed approach.

and with updating the membership $u_{ij}$ and cluster center $c_j$ using the following equations:

$$u_{ij} = \frac{1}{\sum_{n=1}^{c} \left( \left\| \frac{x_i - c_j}{x_i - c_n} \right\| \right)^{\frac{2}{m-1}}} \tag{2}$$

$$c_j = \frac{\sum_{i=1}^{N} u_{ij}^m \cdot x_i}{\sum_{i=1}^{N} u_{ij}^m} \tag{3}$$

The Iterative optimization will stop when

$$\max_{ij} \left\{ \left| u_{ij}^{(k+1)} - u_{ij}^{(k)} \right| \right\} < \varepsilon \tag{4}$$

### 2.2.2. Neutrosophy

The advantage of the neutrosophy is the high noise reduction without image boundary blurring; thus, the result of segmentation is highly improved after the reduction in noise. The neutrosophy represents every pixel in the segmented image by three Neutrosophic constituents: $f$% false, $i$% indeterminate, and $t$% true. The most beneficial component of neutrosophy is that indeterminacy is considered [25].

The pixels of the noise in the panoramic jaw images have a high degree of indeterminacy while the pixels of the lesion region have a low degree of indeterminacy; then, the two groups of pixels can be handled based on the degree of indeterminacy separately. So noise is iteratively reduced and the lesion region is strengthened or untouched. This work explores a novel neutrosophy application by combining Fuzzy C-Means with the domain components of neutrosophy, thus achieving better treatment of the uncertainty data points. Clustering approach is an unsupervised learning approach which is dynamic and adaptive [25].

### 2.2.3. Descriptions of Neutrosophic components for jaw's X-ray image segmentation

In this work, the proposed NFCM approach is applied to solve jaw's X-ray image segmentation problem, where the proposed NFCM is used to determine the lesion from the background in the jaw's X-ray image. This section explains the Neutrosophic pixel and its Neutrosophic components in order to solve jaw's X-ray image segmentation problem as follows:

**Description 1** (*(Neutrosophic set) [28]*). Let $U$ be the universe of the pixels, and $L$ be a foreground set $L \subset U$. A pixel $P$ is represented as p($T'$, $I'$ and $F'$), belongs to A as following: it is $t$% true in the lesion pixel set, $i$% indeterminate, and $f$% false, where $t$ varies in $T'$, $i$ varies in $I'$, and $f$ varies in $F'$. $T'$, $I'$ and $F'$ are standard real subsets of with the range $[-0, 1+]$. For this work $0 \leqslant T' + I' + F' \leqslant 3$.

**Description 2** (*Neutrosophic image*). The image domain of the pixel $P(i, j)$ is transformed into Neutrosophic domain $P_{NS}(i, j) = \{T(i, j), I(i, j), F(i, j)\}$ [29,33], here, $T(i, j)$, $I(i, j)$ and $F(i, j)$ are the probabilities that belong to lesion region, indeterminate and background sets respectively, which are explained as follows:

$$T(i,j) = \frac{\overline{g(\imath,\jmath)} - \bar{g}_{\min}}{\bar{g}_{\max} - \bar{g}_{\min}} \tag{5}$$

$$I(i,j) = 1 - \frac{\mathrm{Ho}(i,j) - \mathrm{Ho}_{\min}}{\mathrm{Ho}_{\max} - \mathrm{Ho}_{\min}} \tag{6}$$

$$F(i,j) = 1 - T(i,j) \tag{7}$$

$$\mathrm{Ho}(i,j) = \mathrm{abs}\left( g(i,j) - \overline{g(\imath,\jmath)} \right) \tag{8}$$

The local mean value is represented by $\overline{g(\imath, \jmath)}$. The homogeneity value of $T$ at $(i, j)$ is represented by $\mathrm{Ho}(i, j)$, which is defined through the absolute value of variance between intensity $g(i, j)$ And its local mean value $\overline{g(\imath, \jmath)}$.

### 2.2.4. Entropy of Neutrosophic (NS) jaw's X-ray image

To evaluate the distribution of different gray level in jaw's X-ray image, entropy of NS was used in this work. Thus, if the entropy is small, the intensities have diverse probabilities and the intensities distribution is non-uniform. If the entropy is the maximum, the different intensities will have similar probabilities and the intensity distribution is uniform.

**Description 3** (*entropy of NS image*). entropy of NS image is explained as the summation of the entropies of three subsets $T$, $I$ and $F$, which is employed in this work to evaluate and measure the elements distribution in the NS domain [29,34].

$$En_T = -\sum P_T(i) \ln P_T(i) \tag{9}$$

$$En_I = -\sum P_I(i) \ln P_I(i) \tag{10}$$

$$En_F = -\sum P_F(i) \ln P_F(i) \tag{11}$$

$$En_{NS} = En_T + En_I + En_F \tag{12}$$

where the entropy of subset $T$ is $En_T$, the entropy of subset $I$ is $En_I$ and the entropy of subset $F$ is $En_F$. The element i probabilities in $T$, $I$ and $F$ are denoted as $P_T(i)$, $P_I(i)$, and $P_F(i)$ respectively. $En_F$ and $En_T$ are employed to measure the elements distribute in NS, and to evaluate the indeterminacy distribution, $En_I$ is utilized.

### 2.2.5. λ-mean operation

The $I(i, j)$ value is employed in order to measure the indeterminate degree of element $P_{ns}(i, j)$. The following equation was used to make subset $I$ correlated with the other subsets $(T, F)$, where the change in both subsets $(T, F)$ affect the element distribution in $I$ and the $I$ entropy.

$$\overline{G}(i,j) = \frac{1}{w * w} \sum_{x=i-w/2}^{i+w/2} \sum_{y=j-w/2}^{j+w/2} G(x,y) \tag{13}$$

where $w$ represented the size of window and $\overline{G}(i,j)$ was the value of intensity. Through the use of the aforesaid equation, an indeterminate pixel (with high indeterminacy) in the background will be progressively integrated into the background, while an indeterminate pixel (with low indeterminacy) inside a lesion will be progressively assimilated into the lesion region.

*2.2.6. A hybrid Neutrosophic sets (NS) with Fuzzy C-Mean clustering (FCM)*

A new clustering approach is proposed in this work based on the hybridization between Neutrosophic sets with Fuzzy C-Mean clustering (NFCM), and the proposed hybridization approach consists of the following steps:

1. Initiate membership matrix $U^l = [u_{wz}]$; the value of $l$ is 0, $w$ represents the pixel index, $z$ represents the cluster index and $l$ represents the number of iteration.
2. $l = l + 1$. Calculate $T^j$, $I^j$ and $F^j$ at each iteration for image $G^j$ using Eqs. (5), (6) and (7).
3. Transform $T^j$, $I^j$ and $F^j$ into vectors $VT$, $VI$ and $VF$.
4. Then, calculate the center vector $L^j = [v_q]$ by $U^j$, $VT$, $VI$ and $VF$.

$$C_v = \frac{\sum_{x=1}^{N} u_{wz}^m \cdot (1 - VI_x) \cdot VT_x \cdot VF_x}{\sum_{x=1}^{N} u_{wz}^m \cdot (1 - VI_x)} \tag{14}$$

where $N$ is the total number of the image pixels, m represents the membership parameter.

5. Update membership matrix $U^{l+1} = [u_{wz}]$ using

$$u_{wz} = \frac{1}{\sum_{d=1}^{C} \left( \left\| \frac{VT_x - C_V}{VT_x - C_d} \right\| \right)^{\frac{2}{m-1}}} \tag{15}$$

where $C$ is the cluster number.

6. $\lambda$-mean operation for $P_{NS}$, $P'_{NS}$ is used to update $G^j$ image which is defined as follows:

$$P'_{NS}(\lambda) = P(T'(\lambda), I'(\lambda), F'(\lambda)) \tag{16}$$

$$T'_{\lambda} = \begin{cases} T & \text{if } I < \lambda \\ T' & \text{if } I \geqslant \lambda \end{cases} \tag{17}$$

$$T'_{\lambda}(i,j) = \frac{1}{w * w} \sum_{x=i-w/2}^{i+w/2} \sum_{y=j-w/2}^{j+w/2} T(x,y) \tag{18}$$

$$F'_{\lambda} = \begin{cases} F & \text{if } I < \lambda \\ F' & \text{if } I \geqslant \lambda \end{cases} \tag{19}$$

$$F'_{\lambda}(i,j) = \frac{1}{w * w} \sum_{x=i-w/2}^{i+w/2} \sum_{y=j-w/2}^{j+w/2} F(x,y) \tag{20}$$

$$I'_{\lambda}(i,j) = 1 - \frac{\mathrm{Ho}'(i,j) - \mathrm{Ho}'_{\min}}{\mathrm{Ho}'_{\max} - \mathrm{Ho}'_{\min}} \tag{21}$$

where $w$ is the window size, $(i, j)$ is the pixel at the window center and $\lambda$ is the threshold of indeterminacy.

7. If $1\|U^{l+1} - U^l\| < \varepsilon$, stop; if not return to step 2.

In this work, $C = 2$ since image has two clusters; $\lambda = 0.1$, $m = 2$ and $w = 5$ where these values were determined experimentally based on the used dataset.

## 3. Results and discussion

To measure the efficiency of the proposed NFCM, we compared it with other segmentation methods, namely; the Hybrid Firefly Algorithm with FCM (FAFCM), and the Artificial Bee Colony with FCM (ABCFCM), these segmentation methods have been employed in this work in order to make a fair comparison with NFCM using the same common criteria and dataset used (real dataset of jaw's panoramic X-ray images), and FAFCM and ABCFCM have been applied in this work as the same way in [31,32]. Since there is no public benchmark and no globally accepted assessment criteria yet, three comprehensive metrics (Area error metrics, specificity and sensitivity metrics) have been used in this work to compare results from different aspects.

### 3.1. Database

In this section, the experiments were performed based on real dataset of jaw's panoramic X-ray images, these dataset consists of 95 jaw's panoramic X-ray images, 60 images have malignant cases and 35 images have benign cases confirmed by pathology. The dataset was collected from the radiology archives of the College of Dentistry and main referral hospitals in the Eastern Province such as King Fahd Hospital of the University and Dammam Central Hospital. The histopathological slides of each lesion have been reviewed by Oral Pathologist to confirm the diagnosis of the radiographic lesion. In this work, 10 panoramic X-ray images have been analyzed for each jaw tumor based on the WHO classification of tumors [35] and jaw lesions according to oral pathology classification of jaw lesions [2]. The boundaries of every lesion in jaw's panoramic X-ray image are delineated by an experienced Oral Pathologist and the manual delineation served as a standard reference.

### 3.2. Evaluation metrics

#### 3.2.1. Area error metrics

To measure how much the Jaw lesion region in the panoramic X-ray image is covered correctly by the generated lesion region and how much is covered incorrectly, the area error metrics were used in this work. Therefore, the area ratio of the false positive (FP), true positive (TP) and false negative (FN) [36] is calculated as following:

$$\mathrm{TP} = \frac{|A_m \bigcap A_a|}{|A_m|} \tag{22}$$

$$\mathrm{FP} = \frac{|A_m \bigcup A_a - A_m|}{|A_m|} \tag{23}$$

$$\mathrm{FN} = 1 - \mathrm{TP} = \frac{|A_m \bigcup A_a - A_a|}{|A_m|} \tag{24}$$

Here, the manually determined lesion region (pixel set) by Oral Pathologist is represented as $A_m$, and the automatically produced lesion region (pixel set) by the proposed approach is represented as $A_a$.

#### 3.2.2. Similarity Index

Similarity Index (SI) was used to measure the closeness of the automatically produced lesion region to the lesion region determined by the Oral Pathologist [25]. The following equation is used to calculate the SI.

$$\mathrm{SI} = \frac{|A_m \cap A_a|}{|A_m \cup A_a|} \tag{25}$$

#### 3.2.3. Specificity

Specificity metric can be used to measure the ability and effectiveness of an algorithm in segmenting or classifying the tissues correctly [37,38]. Thus, the effectiveness of an algorithm in isolating the non-lesion region is represented as specificity. The proposed NFCM segments the non-lesion region of the law's efficiently and the validation results are clearly illustrated in Table 2.

#### 3.2.4. Sensitivity value

Sensitivity value (SV) is used to represent the total number of images that have been correctly segmented and classified [39]. In other words, SV refers to the correctly lesion region identified. The following equation was used to calculate the SV.

$$\mathrm{SV} = \frac{\mathrm{TP}}{\mathrm{TP} + \mathrm{FN}} \tag{26}$$

### 3.3. Compare NFCM with FCM

We compare the proposed NFCM with FCM using the same dataset; the same speckle reduction step is carried out exactly for both NFCM and FCM. Figs. 2 and 3 illustrate the clustered abnormal real jaw's panoramic X-ray images (Periapical–lateral and residual cyst) using the FCM and NFCM respectively.

The resulting images, after applying the FCM and NFCM show the success of the NFCM in determining the lesion region automatically compared with FCM, Figs. 2(c) and 3 (c) show the existence of lesion in the lower jaw using the proposed NFCM which was identical to the manual delineation by Oral Pathologist. The proposed NFCM is able to automatically determine the lesion region and the tumor cells number in the lesion region.

The superiority of NFCM over FCM is that NFCM deals effectively and accurately with indeterminate regions. NFCM integrates the indeterminate pixels (with high indeterminacy) of jaw's panoramic X-ray images into background, while an indeterminate pixel (with low indeterminacy) inside a lesion is progressively assimilated into the lesion region.

But FCM misrecognizes the indeterminate pixels into lesion regions, since FCM uses only the distance to compute the cluster centers, regardless of the indeterminate degree. Moreover, NFCM can analyze the complex jaw's background; then, it can detect the lesion region in the jaw's image.

As shown in Table 1 all the evaluation metrics using the entire database indicate that the proposed NFCM outperformed the FCM by obtaining much better averaging performance. Moreover, for each metric the *P*-value was measured. Statistically, when *P*-value $\leqslant 0.01$, the observed difference is "highly significant", and if the *P*-value $\leqslant 0.05$, the observed difference is "significant". The result of evaluation of the FCM and NFCM shows that the *P*-value for all evaluation metrics is less than 0.005 which means by the statistical criteria that the observed difference is "highly significant". The higher value of TP (enhanced from 83% to 90%) shows that NFCM covers more lesion region compared with FCM. The lower value of FP (decreased from 9.1% to 6.1%) shows that NFCM successfully determined the non-lesion regions compared with FCM.

### 3.4. Compare the NFCM approach with segmentation methods

To measure the efficiency of the proposed NFCM, we compared it with two segmentation methods (FAFCM and ABCFCM), and these segmentation methods have been employed in this work in order to make a fair comparison with NFCM using the same common criteria and dataset used (our

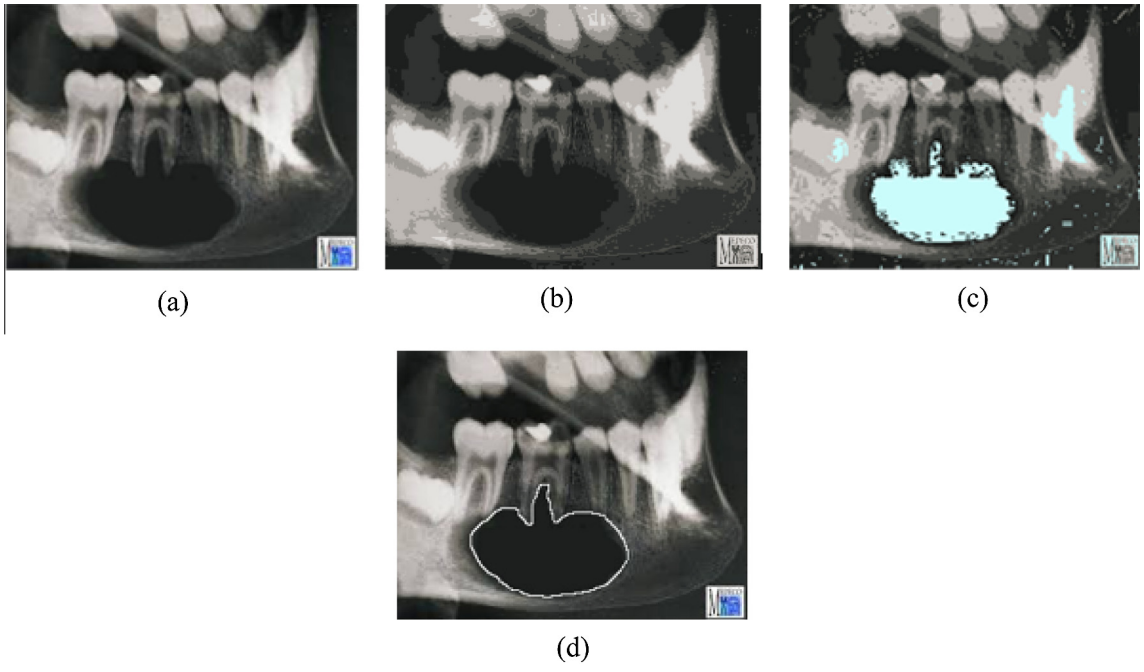


**Figure 2** (a) The original abnormal real jaw's panoramic X-ray images (periapical–lateral and residual cyst), (b) segmented results acquired by FCM, (c) segmented result acquired by the NFCM and (d) manual delineation by Oral Pathologist.

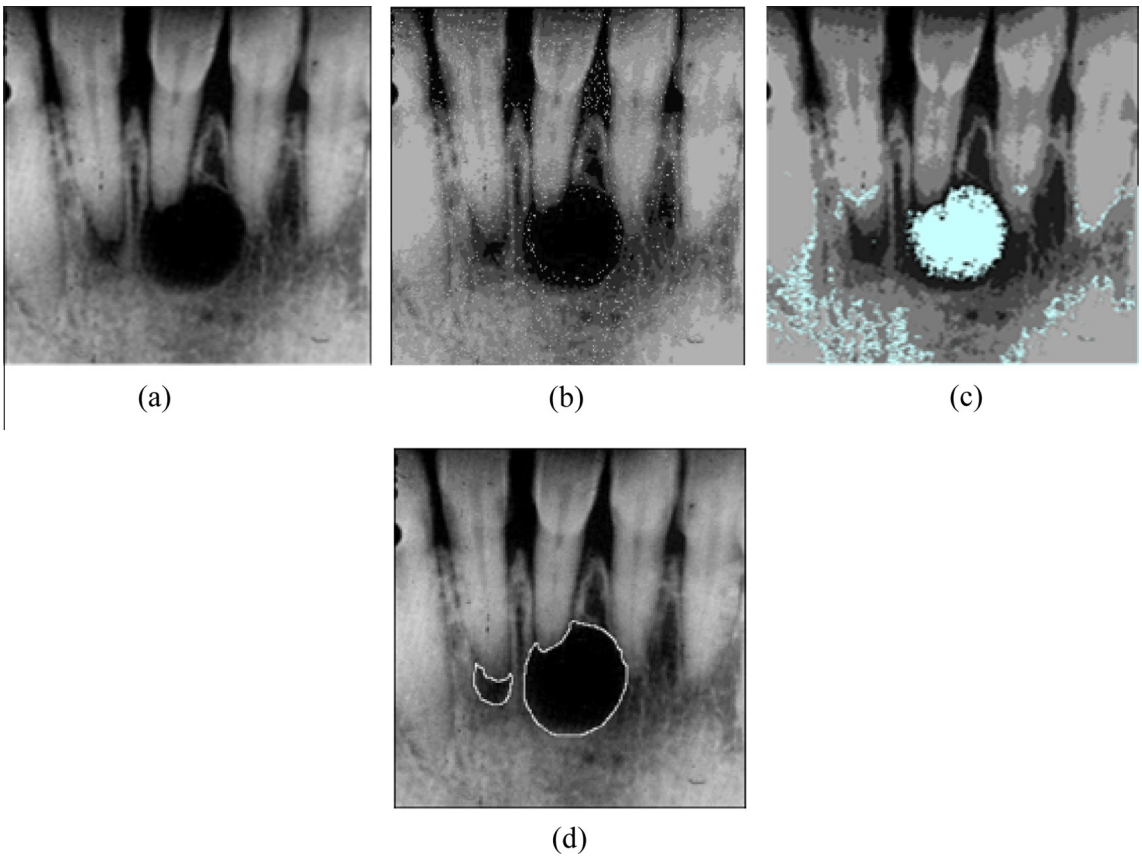


**Figure 3** (a) The original abnormal real jaw's panoramic X-ray images (periapical–lateral and residual cyst), (b) segmented results acquired by FCM, (c) segmented result acquired by the NFCM and (d) manual delineation by Oral Pathologist.

**Table 1** The obtained results from the FCM and the proposed NFCM.

| Average of the area error metrics | | | | |
|---|---|---|---|---|
| Approaches | FP (%) | TP (%) | FN | TN |
| FCM | 9.1 ± 8.5 | 83 ± 5.5 | 17 ± 5.5 | 90.9 ± 8.5 |
| Proposed NFCM | 6.1 ± 5.3 | 90 ± 2.5 | 10 ± 2.5 | 93.9 ± 5.3 |
| *P*-value | < 0.005 | < 0.005 | < 0.005 | < 0.005 |

**Table 2** Comparison results for Similarity Index (SI), sensitivity and specificity values.

| Algorithms | Similarity Index (SI) | Specificity | Sensitivity |
|---|---|---|---|
| FCM | 0.8000 | *0.7723* | *0.8345* |
| ABCFCM | 0.9022 | *0.9122* | *0.925* |
| FAFCM | 0.9313 | *0.9213* | *0.943* |
| NFCM | **0.9471** | ***0.9412*** | ***0.9592*** |

own database). The parameters settings of the firefly algorithm are as follows: number of fireflies ($n = 110$), max iteration = 1000, $\beta = 1$ and $\gamma = 1$, and the parameters settings of the Artificial Bee Colony Algorithm are as follows: cycles number equals 2500 and colony size equals 50 bees. Refer to [31,32] for more details about the FAFCM and ABCFCM methods.

In Fig. 4, the segmentation results of the segmentation methods (ABCFCM and FAFCM) are provided. Fig. 4(a) shows the original abnormal real jaw's panoramic X-ray images (Periapical–lateral and residual cyst), (b) segmented result acquired by FCM, (c) segmented result acquired by the ABCFCM, (d) segmented result acquired by the FAFCM, (e) segmented result acquired by the NFCM and (f) manual delineation by Oral Pathologist, respectively. The lesion regions detected by the proposed NFCM are more accurate and much closer to the Oral Pathologist manual delineation than those of ABCFCM and FAFCM.

Table 2 shows the effectiveness of the proposed NFCM in terms of SI, specificity and sensitivity compared with other methods. For a good and accurate segmentation method, specificity and sensitivity values should be close to 1 [39]. NFCM algorithm dominates the FCM, ABCFCM and FAFCM in terms of specificity and sensitivity and it is obviously demonstrated in Table 3. The proposed NFCM outperformed the other FCM, ABCFCM and FAFCM algorithms as it has SI, specificity and sensitivity values of ***0.9471***, ***0.9412*** and ***0.9592*** respectively. Specificity and sensitivity values are calculated based on the comparison made between the manually determined lesion regions (pixel set) by the Oral Pathologist and the automatically produced lesion region (pixel set) by the proposed algorithms.

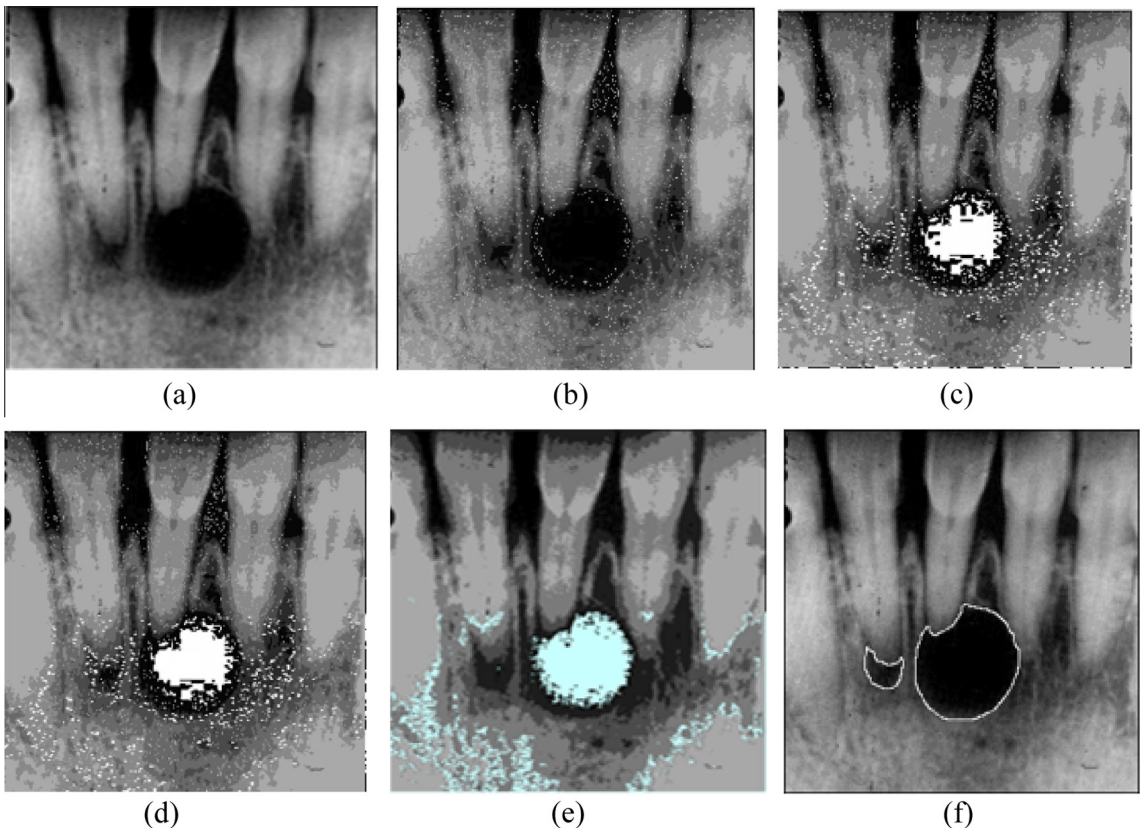


**Figure 4** (a) Is the original abnormal real jaw's panoramic X-ray images (periapical–lateral and residual cyst), (b) segmented result acquired by FCM, (c) segmented result acquired by the ABCFCM, (d) segmented result acquired by the FAFCM, (e) segmented result acquired by the NFCM and (f) manual delineation by Oral Pathologist, respectively.

**Table 3** The performance of the proposed NFCM and the results of other segmentation algorithms (time calculation).

| | Normal image | Abnormal image | | |
|---|---|---|---|---|
| Method | Adults image | Periapical–lateral and residual cyst-1 | Periapical–lateral and residual cyst-2 | Primordial and OKC |
| FCM | 0.41 | 0.47 | 0.48 | 0.51 |
| FAFCM | 0.41 | 0.54 | 0.56 | 0.57 |
| ABCFCM | 0.42 | 0.52 | 0.57 | 0.58 |
| NFCM | **0.46** | **0.57** | **0.59** | **1.02** |

As shown in the Fig. 4, it is clear that the proposed method (NFCM) has better performance if compared with the FCM, FAFCM, and ABCFCM. It has detected the lesion region more accurately. On the other hand, the computation time for the NFCM is higher if compared with the others as shown in Table 3 below.

Table 4 below shows the Number of tumor regions detected (which are real lesions) and number of air gap regions (which are not real lesions) in the upper or lower jaw's panoramic X-ray image using the proposed NFCM.

Moreover; the results obtained using NFCM were compared to other two methods [21,24], where the authors in [24] presented a segmentation system for cyst or tumor cases from dental panoramic images using only 24 panoramic images consisting of various cyst lesions, compared to dataset consisting of 95 jaw's panoramic X-ray images including 10

**Table 4** Number of regions detected (which are real lesions) and number of air gap regions (which are not real lesions) in the upper or lower jaw using the proposed NFCM.

| Image # | Real lesion region | | Air gap region | |
|---|---|---|---|---|
| | Upper jaw | Lower jaw | Upper jaw | Lower jaw |
| 1 | 0 | 2 | 0 | 1 |
| 2 | 0 | 2 | 0 | 0 |
| 3 | 1 | 1 | 0 | 0 |
| 4 | 1 | 0 | 0 | 1 |
| 5 | 1 | 1 | 0 | 0 |
| 6 | 0 | 2 | 0 | 0 |
| 7 | 0 | 1 | 0 | 1 |
| 8 | 0 | 1 | 0 | 0 |
| 9 | 0 | 1 | 1 | 0 |
| 10 | 0 | 1 | 0 | 0 |

types of tumors were used in this work. The authors in [21] introduced a system for the segmentation and classification of abnormal and normal oral cancer images. In both methods [21,24], the tumor region boundaries have been determined using two segmentation methods, where the authors in [24] used Active contour models and the authors in [21] used Marker-Controlled Watershed Segmentation to determine the region of interest (tumor region). These algorithms suffer from many drawbacks such as parameters settings, problems in algorithm initialization, lack of strength to image noise [40,41], which highly affect the final results if inappropriate tumor region is selected. But NFCM algorithm determines and segments the tumor region by indeterminacy degree which is more accurate and robust to image noise. In summary, from the comparisons between NFCM and other segmentation techniques using clustering methods, NFCM has improved the segmentation and detection efficiency of the tumor regions in the real jaw images. The reason behind this improvement is that indeterminacy degree is taken into consideration. So noise is iteratively reduced and the lesion region is strengthened or untouched, since real datasets have a lot of ambiguous data such as noise.

## 4. Conclusion

In this paper, a novel and automatic segmentation approach for panoramic X-ray images has been proposed. It involves speckle noise reduction and NFCM clustering. NFCM is a generalization of FCM which can be useful in pattern classification, data mining, machine learning and other related areas. NFCM was used to segment and determine the lesion region of jaw in panoramic X-ray images which may help in diagnosing jaw lesions. NFCM will help all dentists in diagnosing jaw lesions. NFCM has several advantages which can be summarized as follows: it can be used to segment and find lesion region accurately even in the low-contrast and complicated jaw panoramic X-ray images, it is completely automatic, the proposed NFCM when compared with the ABCFCM and FAFCM produces the most identical lesion region to the manual delineation by the Oral Pathologist, greatly reduced noise without blurring the boundary of the image which significantly improved the segmentation results and shows better performance (FP rate is 6.1%, TP rate is 90%, specificity rate is 0.9412, sensitivity rate is 0.9592 and similarity rate is 0.9471), it has detected the lesion region more accurately and the computation time for the NFCM is higher if compared with other methods. The future work of this research is to develop a classifier that can distinguish malignant and benign lesions of jaw in panoramic X-ray images based on suitable and appropriate features extracted from the segmentation results.

## References

[1] Khosravi N, Razavi SM, Kowkabi M, Navabi AA. Demographic distribution of odontogenic cysts in Isfahan (Iran) over a 23-year period (1988–2010). Dent Res J 2013;10(2):162–7.
[2] Rajendran R. Shafer's textbook of oral pathology. 6th ed, 2009.
[3] Bhadage C, Vaishampayan S, Kolhe S, Umarji H. Osteosarcoma of the mandible mimicking an odontogenic abscess: a case report and review of the literature. Dent Update 2013;40(3):216–21.
[4] Santhosh B. Review on emerging techniques to detect oral cancer. Int J Electr Sci Eng 2015;1(1):41–6.
[5] Sharma N, Om H. Significant patterns for oral cancer detection: association rule on clinical examination and history data. Netw Model Anal Health Inform Bioinform 2014;3(1):1–13.
[6] Weber A. Imaging of cysts and odontogenic tumors of the jaw. Definition and classification. Radiol Clin North Am 1993;31 (1):101–20.
[7] Gundappa M, Ng S, Whaites E. Comparison of ultrasound, digital and conventional radiography in differentiating periapical lesions. Dentomaxillofacial Radiol 2006;35(5):326–33.
[8] White SC. Computer-aided differential diagnosis of oral radiographic lesions. Dentomaxillofacial Radiol 1989;18(2):53–9.
[9] Mileman P, van den Hout W. Evidence-based diagnosis and clinical decision making. Dentomaxillofacial Radiol 2009;38 (1):1–10.
[10] Doi K. Computer-aided diagnosis in medical imaging: historical review, current status and future potential. Comput Med Imag Graph: Off J Comput Med Imag Soc 2007;31(4–5):198–211.
[11] Lin P-L, Lai Y-H, Huang P-W. Dental biometrics: human identification based on teeth and dental works in bitewing radiographs. Pattern Recogn 2012;45(3):934–46.
[12] Neyaz Z, Gadodia A, Gamanagatti S, Mukhopadhyay S. Radiographical approach to jaw lesions. Singapore Med J 2008;49 (2):165–76.
[13] Bernaerts A, Vanhoenacker F, Hintjens J, Chapelle K, De Schepper AM. Imaging approach for differential diagnosis of jaw lesions: a quick reference guide. JBR-BTR 2006;89(1):43–6.
[14] Jamdade A, John A. Bone scintigraphy and panoramic radiography in deciding the extent of bone resection in Benign jaw lesions. J Clin Diagn Res: JCDR 2013;7(10):2351–5.
[15] Gupta S, Grover N, Kadam A, Gupta S, Sah K, Sunitha JD. Odontogenic myxoma. Natl J Maxillofacial Surg 2013;4(1):81–3.
[16] Martins CC, Chalub L, Lima-Arsati YB, Pordeus IA, Paiva SM. Agreement in the diagnosis of dental fluorosis in central incisors performed by a standardized photographic method and clinical examination. Cadernos de Saúde Pública 2009;25:1017–24.
[17] Anuradha K, Sankaranarayanan K. Detection of oral tumor based on marker-controlled watershed algorithm. Int J Comput Appl 2012;52(2).
[18] Dunn JC. A fuzzy relative of the ISODATA process and its use in detecting compact well-separated clusters. J Cybernetics 1973;3 (3):32–57.
[19] Bezdek JC. Pattern recognition with fuzzy objective function algorithms; 1981. p. 256.
[20] Shen S, Sandham W, Granat M, Sterr A. MRI fuzzy segmentation of brain tissue using neighborhood attraction with neural-network optimization. Inf Technol Biomed, IEEE Trans 2005;9(3):459–67.
[21] Anuradha K. Statistical feature extraction to classify oral cancers. J Glob Res Comput Sci 2013;4(2):8–12.
[22] Anuradha K, Sankaranarayanan K. Oral cancer detection using improved segmentation algorithm. Int J Adv Res Comput Sci Softw Eng 2015;5(1):451–6.
[23] Maghsoudi R, Bagheri A, Maghsoudi MT. Diagnosis prediction of lichen planus, leukoplakia and oral squamous cell carcinoma by using an intelligent system based on artificial neural networks. J Dentomaxillofacial Radiol, Pathol Surg 2013;2(2):1–8.
[24] Nurtanio I, Purnama IKE, Hariadi M, Purnomo MH. Cyst and tumor lesion segmentation on dental panoramic images using active contour models. IPTEK J Technol Sci 2011;22(3).
[25] Shan J, Cheng HD, Wang Y. A novel segmentation method for breast ultrasound images based on neutrosophic l-means clustering. Med Phys 2012;39(9):5669–82.
[26] Smarandache F. A unifying field in logics: neutrosophic logic. Neutrosophy, neutrosophic set, neutrosophic probability. 3rd ed. p. 143.
[27] Guo Y, Sengur A. NCM: neutrosophic c-means clustering algorithm. Pattern Recogn 2015;48(8):2710–24.
[28] Cheng HD, Guo Y. A new neutrosophic approach to image thresholding. New Math Nat Comput 2008;04(03):291–308.

Please cite this article in press as: Alsmadi MK, A hybrid Fuzzy C-Means and Neutrosophic for jaw lesions segmentation, Ain Shams Eng J (2016), http://dx.doi.org/10.1016/j.asej.2016.03.016

[29] Anter A, Hassanien A, ElSoud MA, Tolba M. Neutrosophic sets and fuzzy C-means clustering for improving CT liver image segmentation. In: Kömer P, Abraham A, Snášel V, editors. Proceedings of the fifth international conference on innovations in bio-inspired computing and applications IBICA 2014. Springer International Publishing; 2014. p. 193–203.
[30] Trifas AM. Medical image enhancement. Louisiana State University and Agricultural and Mechanical College; 2005.
[31] Alsmadi MK. A hybrid firefly algorithm with fuzzy-C mean algorithm for MRI brain segmentation. Am J Appl Sci 2014;11 (9):1676–91.
[32] Alsmadi MK. MRI brain segmentation using a hybrid artificial bee colony algorithm with fuzzy-C mean algorithm. J Appl Sci 2015;15:100–9.
[33] Mohan J, Yanhui G, Krishnaveni V, Jeganathan K. MRI denoising based on neutrosophic wiener filtering. In: Imaging Systems and Techniques (IST), 2012 IEEE international conference on, 16–17 July 2012. p. 327–31.
[34] Guo Y, Cheng HD, Zhang Y, Zhao W. A new neutrosophic approach to image thresholding. New Math Nat Comput 2008:1–6.
[35] Barnes L, Eveson J, Reichart P, Sidransky D. World Health Organization (WHO) classification of tumors: pathology and genetics of head and neck tumors; 2005.
[36] Liu B, Cheng HD, Huang J, Tian J, Liu J, Tang X. Automated segmentation of ultrasonic breast lesions using statistical texture classification and active contour based on probability distance. Ultrasound Med Biol 2009;35(8):1309–24.
[37] Sikka K, Sinha N, Singh PK, Mishra AK. A fully automated algorithm under modified FCM framework for improved brain MR image segmentation. Magn Reson Imag 2009;27(7):994–1004.
[38] Govindaraj V, Murugan PR. A complete automated algorithm for segmentation of tissues and identification of tumor region in T1, T2, and FLAIR brain images using optimization and clustering techniques. Int J Imag Syst Technol 2014;24(4):313–25.
[39] Khayati R, Vafadust M, Towhidkhah F, Nabavi M. Fully automatic segmentation of multiple sclerosis lesions in brain MR FLAIR images using adaptive mixtures method and markov random field model. Comput Biol Med 2008;38(3):379–90.
[40] Abid Fourati W, Bouhlel MS. Trabecular bone image segmentation using wavelet and marker-controlled watershed transformation. Chin J Eng 2014;2014.
[41] Liew AW-C. Visual speech recognition: lip segmentation and mapping; 2009.

**Dr. Mutasem Khalil Alsmadi** is currently an assistant professor at the Faculty of Applied Studies and Community Service, Department of Management of Information System, University of Dammam. He received his BS degree in Software engineering in 2006 from Philadelphia University, Jordan, his MSc degree in intelligent system in 2007 from University Utara Malaysia, Malaysia, and his PhD in Computer Science from The Notional University of Malaysia. He has published number of papers in the image processing and Algorithm optimization areas. His research interests include Artificial intelligence, Pattern recognition, Algorithms optimization and Computer vision.

Please cite this article in press as: Alsmadi MK, A hybrid Fuzzy C-Means and Neutrosophic for jaw lesions segmentation, Ain Shams Eng J (2016), http://dx.doi.org/10.1016/j.asej.2016.03.016